Investigations on the Diffusion of Platinum between CMSX-4 Superalloy and Platinum-Enriched Bond Coat

Bai, M., Chen, Y. & Xiao, P.

DOI 10.3390/coatings11040441
ESSN 2079-6412

Publisher: MDPI

coatings

MDPI

Article

Investigations on the Diffusion of Platinum between CMSX-4 Superalloy and Platinum-Enriched Bond Coat

Mingwen Bai [1,2,*], Ying Chen [1] and Ping Xiao [1]

[1] Department of Materials, University of Manchester, Manchester M13 9PL, UK; ying.chen-2@manchester.ac.uk (Y.C.); Ping.Xiao@manchester.ac.uk (P.X.)
[2] Institute for Future Transport & Cities, Coventry University, Coventry CV1 5FB, UK
* Correspondence: mingwen.bai@coventry.ac.uk

Abstract: The depletion of Pt in Pt-enriched bond coats due to inter-diffusion with superalloys has been a critical concern for the long-term oxidation resistance of thermal barrier coatings. This study investigated the diffusion behaviour of Pt between CMSX-4 superalloys and two commercial Pt-enriched bond coats comprising intermetallic γ'/γ-phase or β-phase, with the aim to understand the mechanism that leads to the depletion of Pt at high temperatures. The results demonstrated that the diffusion of Pt in superalloy disrupts its phase equilibrium, causes a significant lattice parameter misfit between the γ-phase and γ'-phase, and results in the formation of large γ'-grains with irregular shapes and random orientations. In addition, by using the Thermo-Calc software, Pt was found to have negative chemical interactions with both Al and Ta that stabilise Pt by decreasing its chemical activity. The depletion of Al due to the growth of Al_2O_3 scale during oxidation increases the activity of Pt and therefore accelerates the inwards depletion of Pt towards superalloys.

Keywords: bond coat; platinum; diffusion; thermodynamic; thermal barrier coatings

Citation: Bai, M.; Chen, Y.; Xiao, P. Investigations on the Diffusion of Platinum between CMSX-4 Superalloy and Platinum-Enriched Bond Coat. *Coatings* **2021**, *11*, 441. https://doi.org/10.3390/coatings11040441

Academic Editor: Cecilia Bartuli

Received: 19 March 2021
Accepted: 7 April 2021
Published: 11 April 2021

1. Introduction

Thermal barrier coating systems (TBCs) are widely used in modern gas turbine engines to protect superalloy components. Typical TBCs consist of an oxidation-resistant metallic bond coat and a thermal insulated ceramic topcoat [1]. Electron-beam physical vapour deposition (EBPVD) or air plasma spray (APS) are usually used to deposit a Y_2O_3-stabilised ZrO_2 (YSZ, typically 7 wt.%–8 wt.%) topcoat. Three prevalent types of bond coat are used in the aerospace industry: (I) the NiCoCrAlY system, (II) Pt-aluminide β-phase bond coat, and (III) Pt-diffused γ/γ'-phase bond coat [2]. When exposed to hot gases, an oxidation-resistant α-Al_2O_3 layer forms on the bond coat surface (also known as thermally grown oxide (TGO)) [3]. The adhesion of the TGO layer to the bond coat is crucial to the durability of TBCs during cyclic service, and this has been significantly improved by the addition of Pt because Pt can effectively inhibit the formation of defects (e.g., voids) and the segregation of detrimental impurity (e.g., sulphur) at the oxide/bond coat interface [4–8].

However, severe inter-diffusion between the bond coat and superalloy substrate at elevated temperatures makes it challenging to maintain a high concentration of Pt near the TGO/bond coat interface [8–10]. The oxidation resistance would be significantly undermined by the depletion of Pt, leading to the formation of interfacial cracks and premature TBCs failure [10,11]. As the most direct approach to solve this problem, a thicker Pt layer (>10 μm) is normally applied on the superalloy substrate during the industrial manufacturing process of bond coats to compensate for the inevitable depletion of Pt. Although this is achieved at the price of higher material costs (Pt), longer production times, and greater production costs based on the empirical method of trial and error, the priority is always to minimise the risk of the coatings' premature failure and ensure the long-term TBC durability.

The inter-diffusion problem in β-NiAl and γ′-Ni_3Al inter-metallic alloys has been previously studied [12–21] by a wide range of approaches—e.g., diffusion-couple experiments, thermodynamic calculations, and kinetic calculations. The focus of these studies was mainly on how Pt affects the interdiffusion of Al between bond coats and superalloys to explain the well-observed enhanced oxidation resistance of Pt-enriched bond coats. The experimental results demonstrated that the chemical activity of Al is inversely proportional to the Pt content in a Ni-Pt-Al alloy with a fixed Al content. In other words, Al remains more stable with a higher Pt content in the bond coats. The diffusion of Pt in Ni-based single-crystal superalloys is even more complicated if considering the compositional effect of more than ten alloying elements in Ni-based superalloys [22]. All these alloying elements could affect the chemical activity of Pt individually or synergistically in a positive or negative way to some extent. The lack of a theoretical basis (e.g., thermodynamic and kinetics) for the diffusion of Pt in multi-element material systems makes it even more difficult to find the optimum Pt content for manufacturers. It was reported that the diffusion of Pt into the CMSX-4 substrate induced a significant expansion of the unit cells [23]. As a result, a large biaxial compressive stress is generated which could promote the inwards diffusion of Pt normal to the substrate. In our recent work [24], the depletion of Pt was effectively mitigated in a single-phase Al-enriched γ′-phase coating that was fabricated on the CMSX-4 substrate by the selective γ-phase etching and a subsequent aluminizing process. This has also led to a significantly improved TGO lifetime compared to the industrial-standard dual-phase Pt-diffused γ/γ′ coatings. However, the mechanism behind this achievement, which controls the diffusion of Pt, remains to be revealed.

In this study, the diffusion behaviour of Pt in Pt/superalloy and bond coat/superalloy was systematically investigated, with a focus on the evolution of phase, microstructure, and composition. The mechanism controlling the diffusion behaviour of Pt was also discussed using the CALPHAD method (Computer Coupling of Phase Diagrams and Thermochemistry), aiming to clarify the compositional effect of superalloys on the diffusion of Pt. These findings will shed new light on the approaches to mitigating the depletion of Pt.

2. Materials and Methods

2.1. Sample Preparation

TBCs samples with an average width of 12 mm were sectioned from commercial high-pressure turbine blades comprising a CMSX-4 superalloy substrate, a 7 wt.%–8 wt.% YSZ EBPVD topcoat and two types of Pt-enriched inter-metallic bond coats (β-phase and γ/γ′-phase, respectively). More details on the sample preparation can be found in our previous work (see Figure 3.2 in thesis [25]). Samples were first pre-treated at 1150 °C for 1 h in laboratory air to relieve the residual stress that had been introduced during the coating deposition process and sample handling/sectioning. The TBCs samples were then subjected to an isothermal treatment at 1150 °C for 100 h in laboratory air (CM^{TM} Furnace) and in a vacuum (1×10^{-5} mBar, Edwards Vacuum), respectively. Although it is difficult to completely remove oxygen in the current vacuum condition, the comparison between these two treatments can be used to reveal the oxidation effect on the Pt diffusion.

2.2. Characterization Methods

X-ray diffraction (XRD, Philips X'Pert, Eindhoven, The Netherlands, Cu Kα λ = 0.15405 nm) was used to measure phase compositions at an accelerating voltage of 40 kV and a current of 40 mA. TOPAS software (Bruker, Karlsruhe, Germany, 2005) was employed to calculate the lattice parameters using the Rietveld refinement method. To avoid the effect of the strong (200) texture of a single-crystal superalloy on the Rietveld refinement, a powder sample made of CMSX-4 γ′-cubes was prepared by long-term electrolyte etching to determine the lattice parameters. Cross-sectional microstructure was examined by scanning electron microscopy (SEM, Philip XL30, Eindhoven, The Netherlands). Crystallographic phases were identified by electron backscatter diffraction (EBSD, HKL Nordlys) on SEM (FEI Quanta 650, Lausanne,

Switzerland). An electron probe micro-analyser (EPMA, Cameca, Gennevilliers, France, SX 100, at 20 kV, 100 nA current, 1 μm beam size, and 20 mS dwell time per pixel) was used to analyse the coating compositions on a cross-sectional area of 250 μm × 150 μm.

2.3. Thermodynamic Calculations

Thermo-Calc software (version 4.0) was used to calculate the Ni-Al-X ternary phase diagrams and the chemical activity of Pt and Al in the ternary system. The TCS Ni-based superalloys database (TCNi6) [26] was employed following the well-established CALPHAD technique [27]. The use of the Thermo-Calc software on nickel superalloys and bond coat systems for high-temperature applications has been validated by our previous works [28–30].

3. Results

3.1. Diffusion of Pt into Superalloy

The inwards diffusion of Pt towards superalloys is captured at the early stage of vacuum heat treatment (see Figure 1). An as-electroplated Pt layer on a CMSX-4 superalloy was treated in a vacuum at high temperatures for a very short duration: (A) at 950 °C for 1 min; (B) at 950 °C for 10 min; and (C) at 1150 °C for 10 min. The undulated diffusion front of Pt (dashed lines) indicates the inwards diffusion of Pt towards the superalloy. The original microstructure of CMSX-4 comprising regular and orderly γ′-cubes and γ-matrix was clearly disrupted by the inwards diffusion of Pt, and new Pt-enriched γ′-precipitates (bright areas) with irregular elongated grain microstructures were formed.

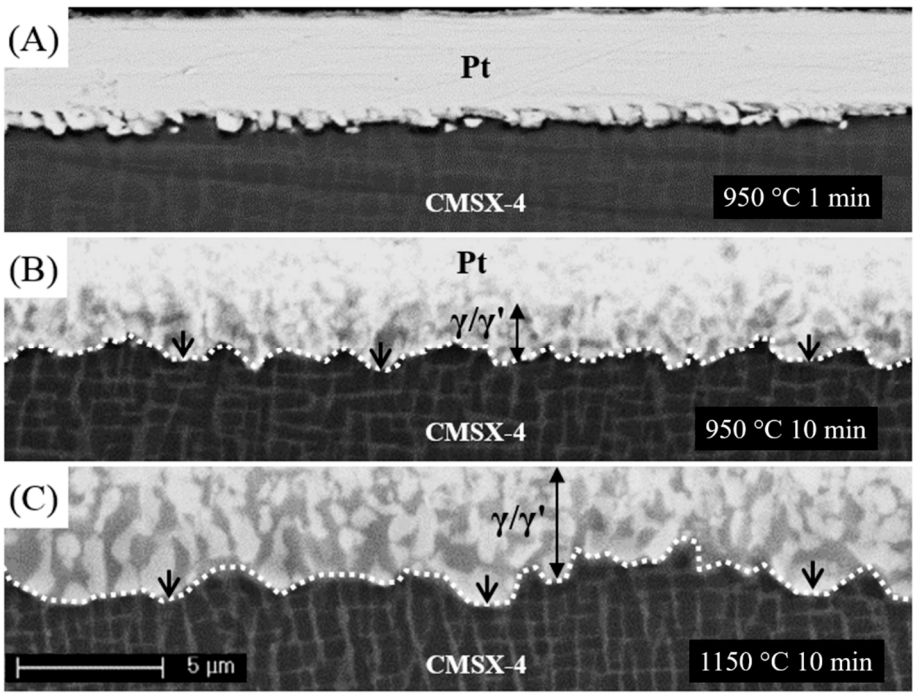

Figure 1. BSE imaging of the cross-sections of an as-electroplated Pt layer on a CMSX-4 after heat treatment in a vacuum: (**A**) 950 °C + 1 min; (**B**) 950 °C + 10 min; and (**C**) 1150 °C + 10 min.

Figure 2 shows that the peak at (200) has a great intensity that even submerges the peak at (111). This strong (200) texture disappeared after Pt diffused into the CMSX-4 superalloy (see Figure 3), which indicates that the inwards diffusion of Pt destroyed its texture and resulted in the formation of new γ′-precipitates with random orientations. In Figure 3, CMSX-4 powder refers to the γ′-cubes that were extracted from the CMSX-4 superalloys by long-term electrolyte etching, and it has random orientations but the same lattice parameter as the CMSX-4 substrate. Significant peak shifts were observed after the vacuum heat treatment, which indicates huge changes in the lattice parameters. This is

mainly caused by the enrichment of Pt in the superalloy, which would expand the unit cell and result in the peak shifting to the left. In addition, the double peaks at (111), (200), and (220) in the Pt-diffused bond coat confirm the uneven enrichment of Pt in γ'-phase and γ-phase.

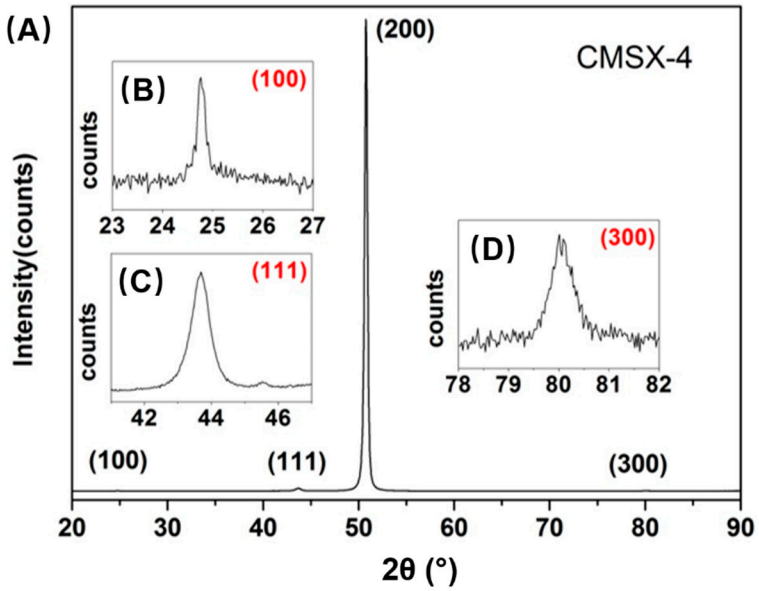

Figure 2. (**A**) XRD pattern of a CMSX-4 superalloy with a strong (200) texture, (**B**) (100) peak, (**C**) (111) peak, and (**D**) (300) peak.

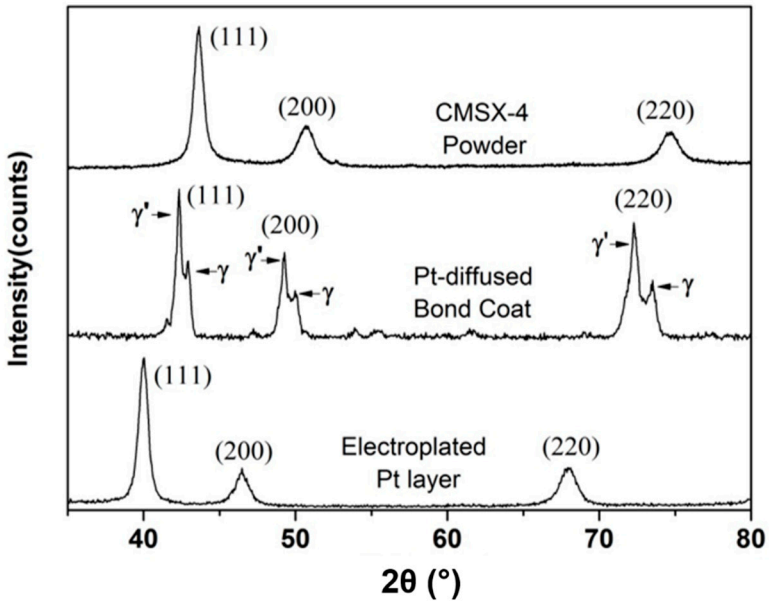

Figure 3. XRD patterns of (top) CMSX-4 powder (γ'-cubes); (middle) as-received Pt-diffused γ/γ' bond coat; and (bottom) as-electroplated Pt layer.

After the vacuum heat treatment, the inwards diffusion of Pt changed the uniform composition of the CMSX-4 substrate (see Figure 4). Ni was depleted in the surface layer, which was substituted by Pt. The inwards diffusion of Pt induced a significant outwards diffusion of Al (Ti and Ta) from the substrate to the surface, which resulted in a depletion zone beneath the Pt-diffused layer. According to the EPMA mappings, the enrichment preference of each alloying element is listed in Table 1.

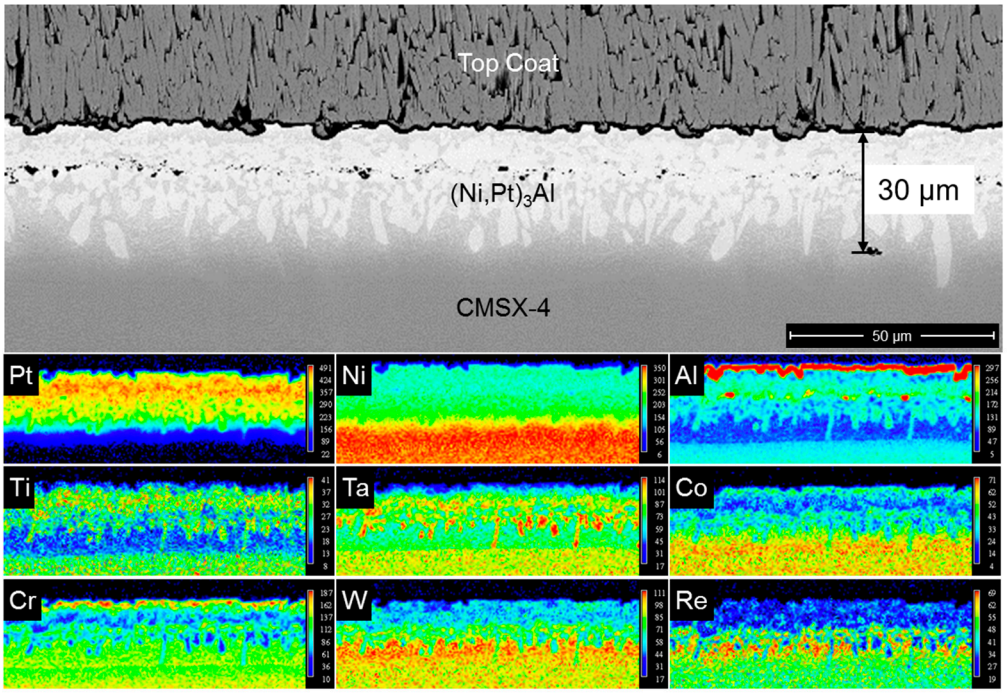

Figure 4. BSE imaging and EPMA mappings of the cross-section of a Pt-diffused γ/γ' bond coat.

Table 1. Main phase and elements in the Pt-diffused γ/γ' bond coat.

γ'-Phase	γ-Phase
$(Ni, Pt)_3X$ (X = Al, Ti or Ta)	Ni (Cr, Co, W, Re)

3.2. Diffusion of Pt in γ/γ' Bond Coat/Superalloy

Figure 5 shows the phase and microstructural evolution of the Pt-diffused γ/γ' bond coat during oxidation. The EBSD colour maps show the morphology and orientations of the grains in the Pt-diffused γ/γ' bond coat. It is observed that the as-received Pt-enriched layer comprises large grains with irregular shapes and random orientations, while the CMSX-4 single-crystal superalloy underneath shows a single orientation. This agrees well with the XRD pattern obtained from the Pt-diffused bond coat surface, indicating that the enrichment of Pt destroyed the microstructure of the single-crystal superalloy and resulted in new precipitates with random orientations. These randomly orientated grains mainly consist of γ'-phase with a minor incorporation of γ-phase, and the size of these grains increases with the oxidation time. Based on the EBSD grain size analysis, the diameter of the grains increased from 2.2 $\pm$ 1.4 μm (as-received) to 5.5 $\pm$ 3.0 μm (40 h) and 5.8 $\pm$ 4.1 μm (100 h), respectively. The formation of these enlarged grains is accompanied by an enrichment of Pt and γ'-phase elements, including Al, Ti, and Ta. During oxidation, significant grain growth was observed stretching towards the substrate, and the average thickness of the Pt-diffused layer increased from 26 to 69 μm. In addition, crystal twinning (growth twin) was observed in some grains at the diffusion fronts. The formation of these growth twins indicates an interruption or change in the lattice during the grain growth.

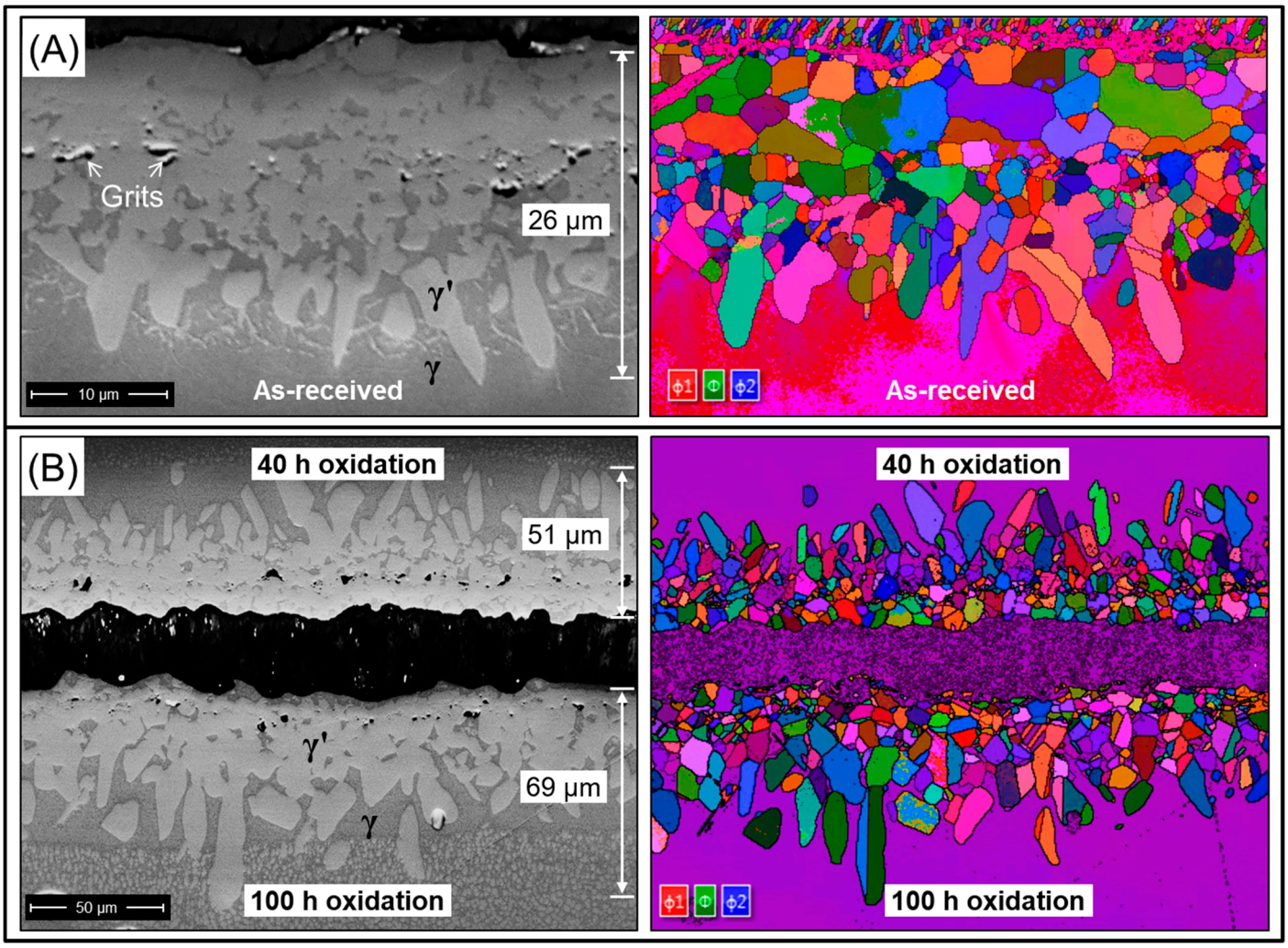

Figure 5. BSE imaging and EBSD Euler colour mapping of the cross-section of a Pt-diffused γ/γ' bond coat: (**A**) as-received; and (**B**) after oxidation at 1150 °C for 40 h (top) and 100 h (bottom).

Figure 6 shows the concentration profiles of Pt and Al on the cross-sections of the Pt-diffused γ/γ' bond coat after 100 h heat treatments. The drop in the Pt peak near the TGO/bond coat interface indicates a significant inwards diffusion of Pt towards the substrate. The oxidation treatment greatly accelerates the inwards diffusion of Pt in comparison with that which had been treated in a vacuum. It is also observed that the diffusion of Al occurs in an opposite direction with Pt. An outwards diffusion of Al is seen after both heat treatments in which the Al content near the surface is even higher than the as-received bond coat, while Al is depleted in the substrate with a significant drop of Al from ~5.6 wt.% to ~4 wt.%.

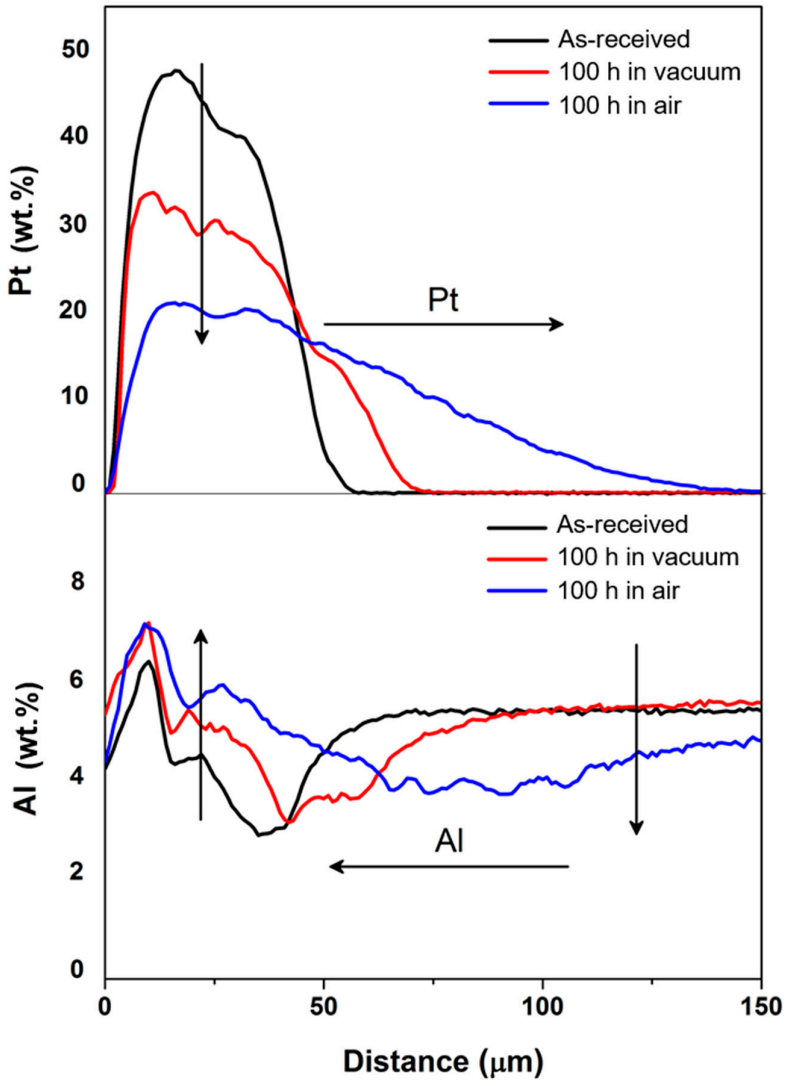

Figure 6. Pt and Al concentrations on the cross-sections of Pt-diffused γ/γ' bond coat.

3.3. Diffusion of Pt in β Bond Coat/Superalloy

Figure 7 shows the evolution of the phase and microstructure of the standard Pt-aluminide β bond coat after long-term diffusion and oxidation. As indicated by the EBSD phase maps, a coherent β-phase layer is observed in the as-received Pt-aluminide β bond coat, which remains the same after 100 h in a vacuum. After 100 h in air, the γ'-phase is observed segregating at the grain boundaries of β-phase. The formation of γ'-phase after oxidation is mainly caused by the depletion of Al due to the growth of Al_2O_3 scale and the inwards diffusion of Al towards superalloys. Detailed EPMA mappings can be found in Figure 8, and the concentration profiles of Pt and Al are plotted in Figure 9. A significant decrease in Al content is seen in the bond coat area from ~20 wt.% to ~15 wt.% after heat treatment in both air and vacuum, while an increase is also observed in the superalloy from ~5 wt.% to ~7 wt.%. This indicates an inwards diffusion of Al, which is exactly the opposite of that of Al in the Pt-diffused γ/γ' bond coat (see Figure 6). In addition, the Pt content drops from ~40 wt.% to ~15 wt.% after both heat treatments, indicating an inward diffusion of Pt, which is accompanied by the similar diffusion of Al towards superalloy. In the as-received β bond coat, Pt is initially enriched in the outer β-phase layer near the TGO/bond coat interface, which also contains a significantly high content of Al. After 100 h in a vacuum, both Pt and Al are uniformly distributed in the β-phase. After 1150 °C 100 h in air, it is observed that Pt and Al are both enriched in β-phase rather than the γ'-phase, which indicates that Pt is relatively more stable in the β-phase than in the γ'-phase.

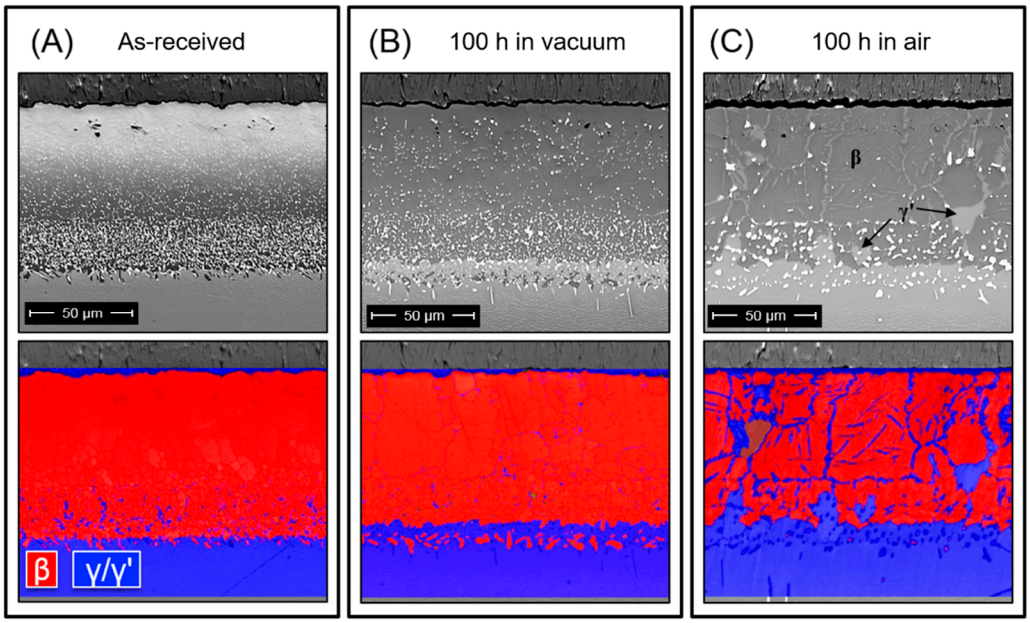

Figure 7. BSE imaging (top) and EBSD phase mapping (bottom) of the Pt-aluminide β bond coat: (**A**) As-received; (**B**) 100 h in vacuum; (**C**) 100 h in air.

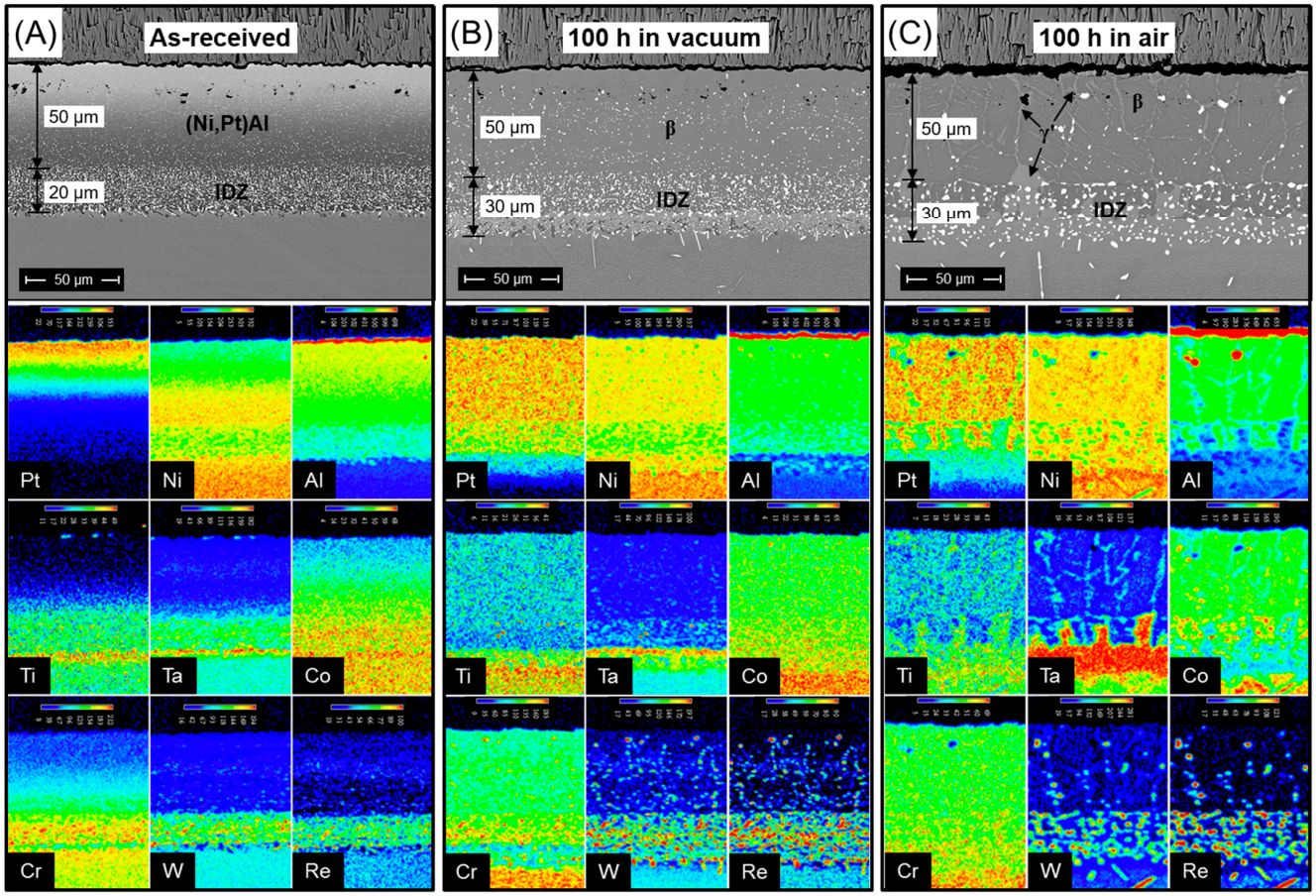

Figure 8. BSE imaging and EPMA mapping of the cross-section of the Pt-aluminide β-phase bond coat: (**A**) As-received; (**B**) 100 h in vacuum; (**C**) 100 h in air.

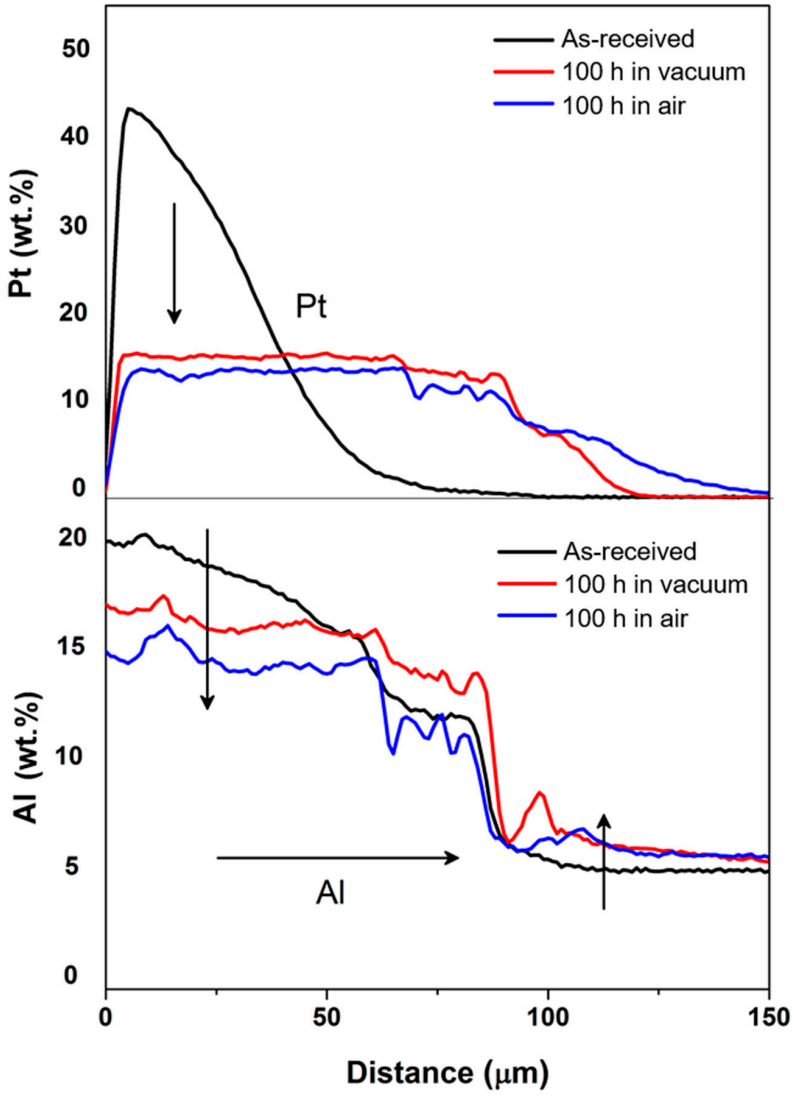

Figure 9. Pt and Al concentrations on the cross-sections of Pt-aluminide β bond coats.

From the EPMA mappings, alloying elements also show distinctive enrichment preferences in the Pt-aluminide β bond coat, which are listed in Table 2. Cr and Co are uniformly enriched in β-phase in the same way as Pt and Al, but the content of Cr and Co is much lower than that of the superalloys. Ti and Ta are no longer co-enriched with Pt and Al. The enrichment of these alloying elements could also affect the diffusion of Pt in intermetallic phases; the mechanisms will be discussed by thermodynamic calculations.

Table 2. Main phase and elements in the Pt-aluminide β bond coat.

β-Phase	Γ′-Phase	γ-Phase
(Pt, Ni, Cr, Co) Al	Ni_3X (X = Ti, Ta)	Ni (W, Re, Cr, Co)

4. Discussion

In an as-received CMSX-4 single-crystal superalloy after standard heat treatment (SHT), the γ/γ' phase interface remains coherent with a cube-cube orientation relationship between the γ' precipitates and γ matrix [31]. To keep the lowest interfacial energy, the coherency of the γ/γ' phase interface is critically dependent on the lattice misfit δ between the γ-phase and γ'-phase, which is defined according to the following equation,

$$\delta = 2 \times \left[\frac{a_{\gamma'} - a_{\gamma}}{a_{\gamma'} + a_{\gamma}} \right]. \quad (1)$$

An increase in the magnitude of δ would induce the loss of coherency at the γ/γ' interface, which would then lead to the coarsening of γ'-precipitates.

Since Pt has a larger atomic radius than Ni [32], the enrichment of Pt in γ'-Ni_3Al by substituting Ni would therefore induce an expansion of the unit cell. It results in an increased lattice parameter of γ'-phase (Table 3). The lattice parameter of γ'-phase is 1.5% larger than the γ-phase, which will cause a significant lattice misfit and lead to loss of coherency at the interface between the γ-phase and γ'-phase. As a result, the γ'-cubes will coarsen and grow to minimise the interfacial energy by decreasing the phase interface.

Table 3. Lattice parameters a (Å) calculated from XRD patterns.

Sample	*a* (Å)
CMSX-4 superalloy	3.594
CMSX-4 (γ'-cubes)	3.597
As-electroplated Pt layer	3.908
Pt-diffused γ'/γ bond coat	$a(\gamma)$ = 3.643; $a(\gamma')$ = 3.698

The enrichment of Pt in CMSX-4 by substituting Ni would also induce a phase disequilibrium in thermodynamic stability, which results in a redistribution of the γ-phase and γ'-phase (see Figure 10). Based on the Thermo-Calc calculation, Pt-based superalloy refers to a new system, if we assume Ni atoms in the Ni-based superalloy are completely replaced by Pt atoms so that Pt has an equal atomic stoichiometric with Ni. From the curves, it is observed that the temperature for the phase inversion between the γ'-phase and γ-phase (i.e., the temperature when their phase fraction is the same) in the Pt-based superalloy has increased by over 200 °C. This huge difference in the dependency of temperature on the amount of γ'-phase between Pt-based and Ni-based superalloys will cause a disruptive impact on the phase equilibrium at high temperatures, leading to the formation of a higher content of the γ'-phase in the Pt-diffused layer at 1150 °C during vacuum heat treatment.

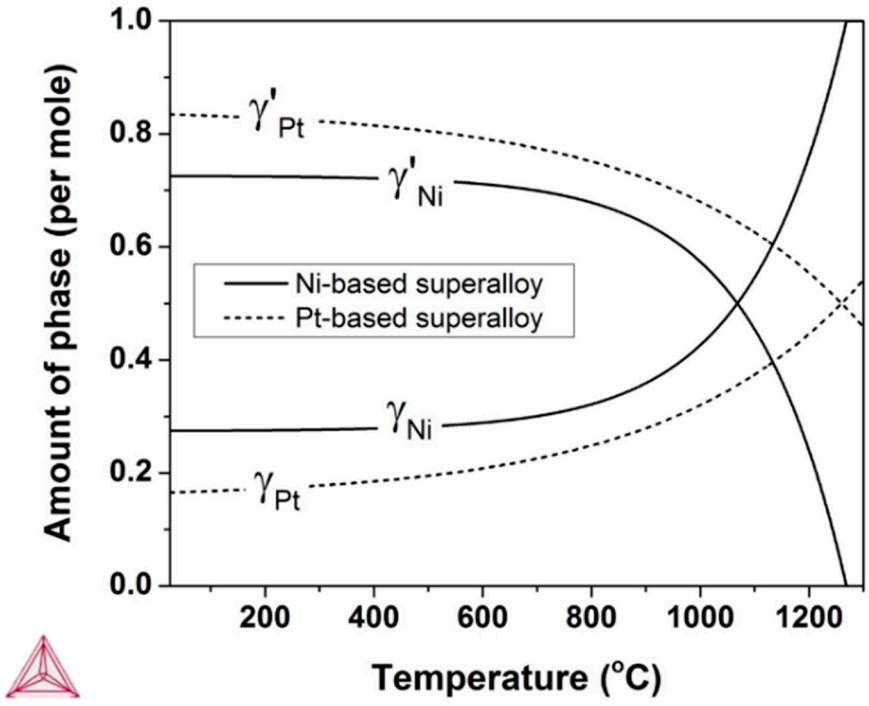

Figure 10. Phase compositions of Ni-based and Pt-based superalloy as a function of temperature.

The diffusion of Pt in a metallic solid solution is mainly determined by its chemical potential μ, which can be expressed by thermodynamic activity *a*, which is equivalent to the 'effective concentration' of an alloying element in a solid solution.

Figure 11 shows the chemical activity of Pt in the Ni-Pt-Al ternary system at 1150 °C. as calculated by the Thermo-Calc software. It is observed that the Pt activity is lowest in β-phase with addition of 50 at.% Al, that when Pt content is 50 at.%, the Pt activity in β-phase is 1.28×10^{-6}, which is one order of magnitude lower than γ′-phase (1.37×10^{-5}) and two orders of magnitude lower than γ-phase (1.49×10^{-4}). In other words, even though the Pt content in the three phases is the same as 50 at.%, the effective concentration of Pt in β-phase is one order of magnitude lower than γ′-phase and two orders of magnitude lower than γ-phase, which means the lowest tendency for the depletion of Pt in β-phase. Accordingly, Pt is most stable in the β-phase, less stable in the γ′-phase, and least stable in the γ-phase. On the other hand, the phase transformation from the γ′-phase to the γ-phase and from the β-phase to the γ′-phase, due to the depletion of Al, would result in both a higher activity of Pt and a large tendency to diffuse away. The depletion of Al normally occurs due to the growth of Al_2O_3 layer, which would therefore accelerate the depletion of Pt.

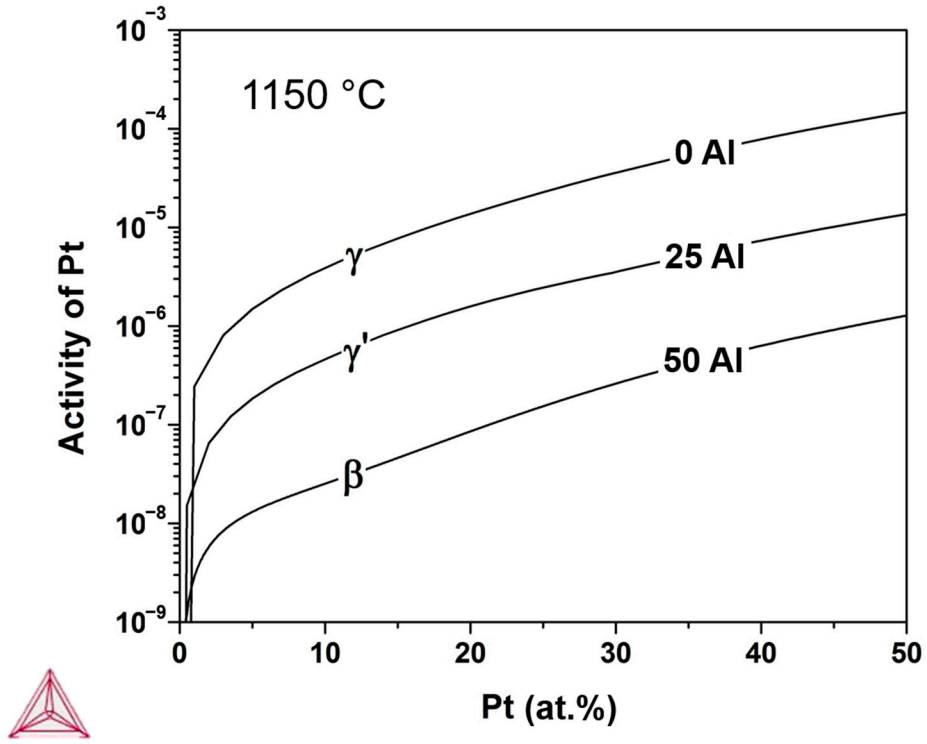

Figure 11. Chemical activity of Pt in the Ni-Pt-Al system at 1150 °C.

Other alloying elements may also determine the diffusion of Pt by affecting its chemical activity. Figure 12 shows the Ni-Al-X ternary phase diagrams at 1150 °C. According to the shape of the γ′-phase area, Co promotes the γ′-phase mainly by substitutions of Ni, while Ti and Ta promote the formation of the γ′-phase mainly by the substitution of Al. For Cr, a mixed behaviour is observed, which means that there is no preference for the substitute.

Figure 13 shows the effect of other alloying elements on the chemical activity of Pt in the β-PtX and γ′-Pt_3X binary systems at 1150 °C. The chemical activity of Pt is significantly decreased by the addition of Al and Ta, which indicates a similar negative chemical interaction with Pt. Ta is also enriched in the γ′-phase in the Pt-diffused γ/γ′ bond coat, so it would further stabilise Pt in the γ′-phase by reducing the activity of Pt.

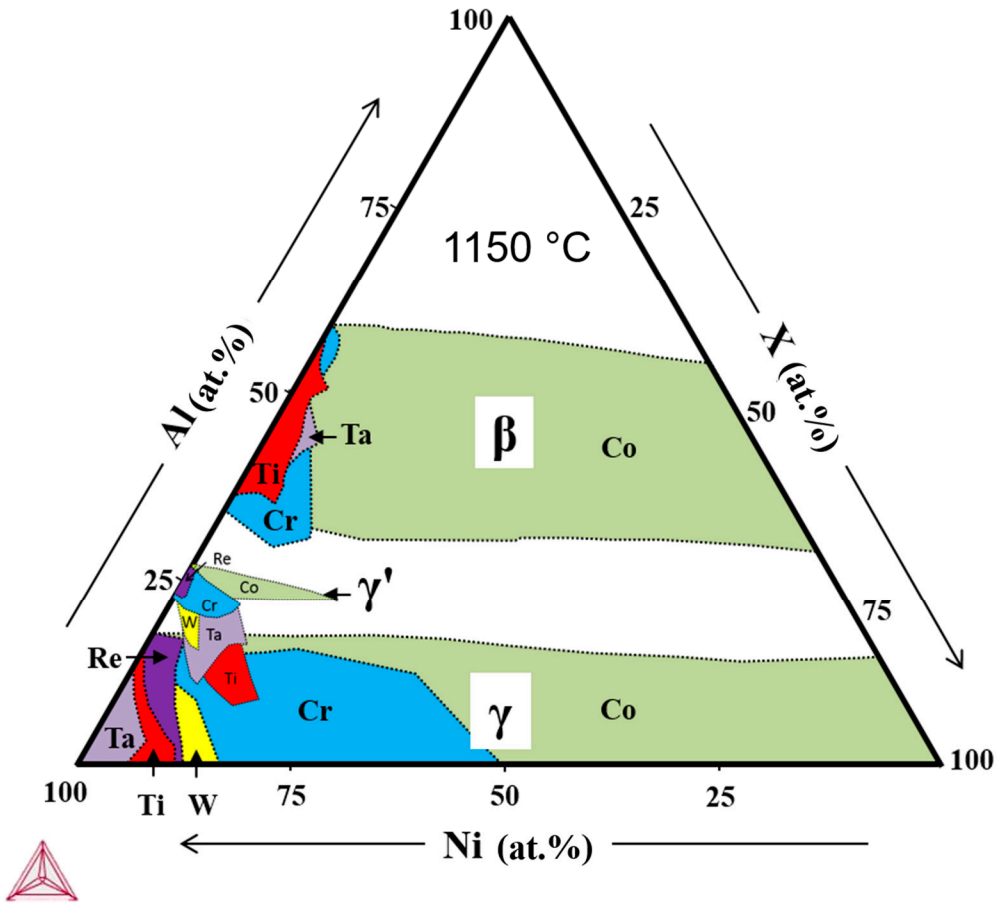

Figure 12. Ni-Al-X ternary phase diagrams (overlayed) at 1150 °C.

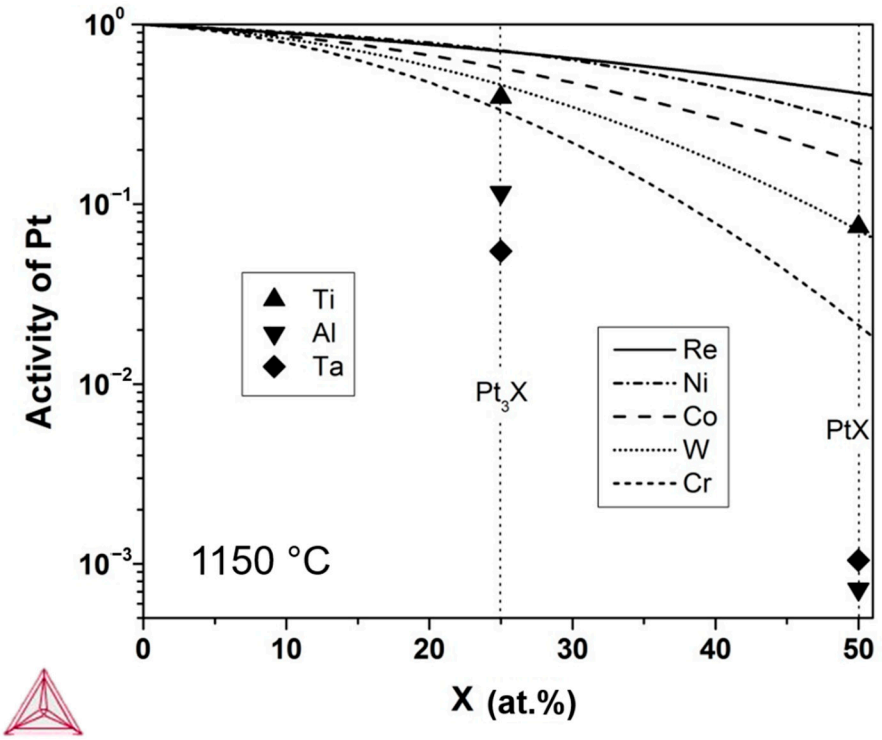

Figure 13. Chemical activity of Pt in the PtX and Pt_3X binary systems at 1150 °C.

5. Conclusions

The diffusion of Pt in the CMSX-4 superalloys has caused significant changes in the phase, microstructure, and compositions. By substituting Ni atoms, the enrichment of Pt in the γ'-phase caused a lattice parameter misfit between the γ-phase and γ'-phase, which led to a severe coarsening of the γ'-phase and resulted in the formation of large γ'-grains with irregular shapes and random orientations. During oxidation, the depletion of Pt is more significant in the Pt-diffused γ/γ' bond coat with an outwards diffusion of Al from superalloys to bond coats, in comparison with the Pt-aluminide β bond coat with an inwards diffusion of Al. Thermodynamic calculations reveal that Pt is most stable in the β-phase, less stable in the γ'-phase, and least stable in the γ-phase. Pt has negative chemical interactions with Al and Ta, which could stabilise Pt by decreasing its chemical activity. The depletion of Al due to the growth of Al_2O_3 scale during oxidation would increase the chemical activity of Pt and therefore accelerate the inwards depletion of Pt towards superalloys.

Author Contributions: Conceptualization, M.B. and Y.C.; methodology, M.B.; software, M.B.; writing—review and editing, M.B., Y.C., and P.X.; supervision and project administration, P.X. All authors have read and agreed to the published version of the manuscript.

Funding: This research received no external funding.

Institutional Review Board Statement: Not applicable.

Informed Consent Statement: Not applicable.

Data Availability Statement: Not applicable.

Acknowledgments: The authors would like to thank Brian Ralph for proof reading, Andy Wallwork, and John Charnock for the experimental assistance. The authors would also like to acknowledge David Rickerby from Rolls-Royce for the supply of the TBC sample.

Conflicts of Interest: The authors declare no conflict of interest.

References

1. Evans, A.G.; Mumm, D.R.; Hutchinson, J.W.; Meier, G.H.; Pettit, F.S. Mechanisms controlling the durability of thermal barrier coatings. *Prog. Mater. Sci.* **2001**, *46*, 505–553. [CrossRef]
2. Nicholls, J.R. Advances in coating design for high-performance gas turbines. *MRS Bull.* **2003**, *28*, 659–670. [CrossRef]
3. Clarke, D.R.; Levi, C.G. Materials design for the next generation thermal barrier coatings. *Annu. Rev. Mater. Res.* **2003**, *33*, 383–417. [CrossRef]
4. Zhang, Y.; Haynes, J.A.; Wright, G.; Pint, B.A.; Cooley, K.M.; Lee, W.Y.; Liaw, P.K. Effects of Pt incorporation on the isothermal oxidation behavior of chemical vapor deposition aluminide coatings. *Met. Mater. Trans. A* **2001**, *32*, 1727–1741. [CrossRef]
5. Cadoret, Y.; Bacos, M.P.; Josso, P.; Maurice, V.; Marcus, P.; Zanna, S. Effect of Pt additions on the sulfur segregation, void formation and oxide scale growth of cast nickel aluminides. *Mater. Sci. Forum* **2004**, *461–464*, 247–254. [CrossRef]
6. Haynes, J.A.; Pint, B.A.; More, K.; Zhang, Y.; Wright, I.G. Influence of sulfur, platinum, and hafnium on the oxidation behavior of cvd nial bond coatings. *Oxid. Met.* **2002**, *58*, 513–544. [CrossRef]
7. Hou, P.; Mccarty, K.F. Surface and interface segregation in β-NiAl with and without Pt addition. *Scr. Mater.* **2006**, *54*, 937–941. [CrossRef]
8. Chen, J.; Little, J. Degradation of the platinum aluminide coating on CMSX4 at 1100 °C. *Surf. Coat. Technol.* **1997**, *92*, 69–77. [CrossRef]
9. Bouchet, R.; Mévrel, R. Influence of platinum and palladium on diffusion in β-NiAl phase. *Defect Diffus. Forum* **2005**, 238–243. [CrossRef]
10. Zhao, X.; Liu, J.; Rickerby, D.; Jones, R.; Xiao, P. Evolution of interfacial toughness of a thermal barrier system with a Pt-diffused γ/γ' bond coat. *Acta Mater.* **2011**, *59*, 6401–6411. [CrossRef]
11. Hayashi, S.; Sordelet, D.J.; Walker, L.R.; Gleeson, B. Interdiffusion in Pt-containing γ-ni and γ'-ni3al alloys at 1150 °C. *Mater. Trans.* **2008**, *49*, 1550–1557. [CrossRef]
12. Minamino, Y.; Koizumi, Y.; Tsuji, N.; Morioka, M.; Hirao, K.; Shirai, Y. Pt diffusion in B2-type ordered NiAl intermetallic compound and its diffusion mechanisms. *Sci. Technol. Adv. Mater.* **2000**, *1*, 237–249. [CrossRef]
13. Yamane, T.; Hisayuki, K.; Yoshida, H.; Minamino, Y.; Araki, H.; Hirao, K. Diffusion of platinum, vanadium and manganese in Ni_3Al phase under high pressure. *J. Mater. Sci.* **1999**, *34*, 1835–1838. [CrossRef]

14. Bouchet, R.; Mevrel, R. Calculating the composition-dependent diffusivity matrix along a diffusion path in ternary systems. *Calphad* **2003**, *27*, 295–303. [CrossRef]
15. Copland, E. Partial Thermodynamic properties of γ'-(Ni,Pt)3Al in the Ni-Al-Pt system. *J. Phase Equilibria Diffus.* **2007**, *28*, 38–48. [CrossRef]
16. Filipek, R.; Datta, P.K.; Danielewski, M.; Bednarz, L.; Best, R.; Rakowska, A. *Interdiffusion in the Pt/Beta-NiAl System*; Scitec Publications Ltd.: Uetikon-Zuerich, Switzerland, 2001; Volume 194-1, pp. 571–576.
17. Gleeson, B.; Wang, W.; Hayashi, S.; Sordelet, D. Effects of platinum on the interdiffusion and oxidation behavior of Ni-Al-based alloys. In *High Temperature Corrosion and Protection of Materials 6, Prt 1 and 2, Proceedings*; Steinmetz, P., Wright, I.G., Meier, G., Galerie, A., Pieraggi, B., Podor, R., Eds.; Trans Tech Publications Ltd.: Zurich-Uetikon, Switzerland, 2004; Volume 461–464, pp. 213–222.
18. Hayashi, S.; Ford, S.; Young, D.; Sordelet, D.; Besser, M.; Gleeson, B. α-NiPt(Al) and phase equilibria in the Ni–Al–Pt system at 1150 °C. *Acta Mater.* **2005**, *53*, 3319–3328. [CrossRef]
19. Matsumaru, H.; Hayashi, S.; Narita, T. Interdiffusion between Ni based superalloy and diffusion barrier coatings at 1423 K. *Mater. Sci. Forum* **2006**, *522–523*, 285–292. [CrossRef]
20. Karunaratne, M.; Reed, R. Interdiffusion of the platinum-group metals in nickel at elevated temperatures. *Acta Mater.* **2003**, *51*, 2905–2919. [CrossRef]
21. Chen, Y.; Zhao, X.; Bai, M.; Chandio, A.; Wu, R.; Xiao, P. Effect of platinum addition on oxidation behaviour of γ/γ' nickel aluminide. *Acta Mater.* **2015**, *86*, 319–330. [CrossRef]
22. Reed, R.C. *The Superalloys: Fundamentals and Applications*; Cambridge University Press: Cambridge, UK, 2008.
23. Zhao, X.; Cernik, B.; Tang, C.; Thompson, S.; Xiao, P. Stress evolution in a Pt-diffused γ/γ' bond coat after oxidation. *Surf. Coat. Technol.* **2014**, *247*, 48–54. [CrossRef]
24. Liu, C.; Chen, Y.; Qiu, L.; Liu, H.; Bai, M.; Xiao, P. The al-enriched γ'-Ni_3Al-base bond coat for thermal barrier coating applications. *Corros. Sci.* **2020**, *167*, 108523. [CrossRef]
25. Bai, M. *Fabrication and Characterization of Thermal Barrier Coatings*; University of Manchester: Manchester, UK, 2015.
26. *TCS Ni-Based Superalloys Database, version 6.0*; Software For thermodynamic calculation; Foundation of Computational Thermodynamics: Stockholm, Sweden, 2011.
27. Andersson, J.-O.; Helander, T.; Höglund, L.; Shi, P.; Sundman, B. Thermo-Calc & DICTRA, computational tools for materials science. *Calphad* **2002**, *26*, 273–312. [CrossRef]
28. Bai, M.; Reddy, L.; Hussain, T. Experimental and thermodynamic investigations on the chlorine-induced corrosion of HVOF thermal sprayed NiAl coatings and 304 stainless steels at 700 °C. *Corros. Sci.* **2018**, *135*, 147–157. [CrossRef]
29. Pala, Z.; Bai, M.; Lukac, F.; Hussain, T. Laser clad and HVOF-sprayed stellite 6 coating in chlorine-rich environment with KCl at 700 °C. *Oxid. Met.* **2017**, *88*, 749–771. [CrossRef]
30. Bai, M.; Song, B.; Reddy, L.; Hussain, T. Preparation of MCrAlY–Al_2O_3 composite coatings with enhanced oxidation resistance through a novel powder manufacturing process. *J. Therm. Spray Technol.* **2019**, *28*, 433–443. [CrossRef]
31. Reed, R.C. *The Superalloys: Fundamentals and Applications*; Cambridge University Press: Cambridge, UK, 2006.
32. Teatum, E.T.; Gschneidner, K.A., Jr.; Waber, J.T. *Compilation of Calculated Data Useful in Predicting Metallurgical Behavior of the Elements in Binary Alloy Systems*; Los Alamos Scientific Laboratory of the University of California: Santa Fe, NM, USA, 1960; Volume 2345.